Trapping thresholds in ordinary site percolation

Lincoln Paterson
Australian Petroleum Cooperative Research Centre, CSIRO Division of Petroleum Resources, P.O. Box 3000, Glen Waverley, Vic 3150, Australia

(Received 12 August 1998)

Numerical estimates for percolation trapping thresholds in two- and three-dimensional ordinary site percolation are calculated. Threshold estimates are square 0.396, triangular 0.490, diamond 0.529, simple cubic 0.658, body-centered cubic 0.727, and face-centered cubic 0.780, with estimated accuracy better than ± 0.002. These are all slightly less than one minus the corresponding ordinary percolation thresholds (without trapping). These trapping thresholds appear to be described by the universal formula proposed by Galam and Mauger for ordinary percolation thresholds. [S1063-651X(98)12812-X]

PACS number(s): 64.60.Ak, 47.55.Mh

I. INTRODUCTION

Percolation with trapping is important because of its relevance to the trapping of residual fluids in slow capillary dominated displacements in porous media. Residual fluid saturation is a critical parameter to the economics of petroleum reservoirs. A description of percolation with trapping can be found in several textbooks [1–5]. Percolation with trapping exists in two varieties: ordinary and invasion.

In 1983 estimates of thresholds in percolation with trapping were provided by Wilkinson and Willemsen [6]. They studied invasion percolation with trapping on triangular, square, and honeycomb lattices in two dimensions, but only the simple-cubic lattice in three dimensions. They observed that the simple-cubic lattice gives a constant value of the fraction of invading phase of $p_t \sim 0.66$ as the lattice size $L \to \infty$. This corresponds to a defender fraction of 0.34, which they noted was close to but significantly different from the percolation threshold $p_c = 0.3116$ for the same lattice. Invasion percolation with trapping on the two-dimensional (2D) lattices produces power-law behavior, with the fraction of invading phase tending toward zero as $L \to \infty$.

Trapping was extended to ordinary percolation by Dias and Wilkinson [7] without providing numerical estimates of threshold values. At that time, interest was concentrated on cluster size distributions and the universality of critical exponents, and whether trapping created a different class. The evidence supported a negative conclusion.

Since then, estimates of trapping thresholds have been neglected, especially in three dimensions. A reason for this is that the trapping mechanism necessarily involves much larger amounts of computational effort than ordinary percolation thresholds as it is necessary to check for trapping as each site is added. Pokorny *et al.* [8] have made an estimate for bond percolation with trapping on the square network at $p_t \approx 0.520$. The ordinary percolation threshold p_c (bond) without trapping for the square lattice is exactly 0.5 [9]. Here $p_t + p_c > 1$, but Pokorny *et al.*, use a different definition of p_t from the one used here, and by Wilkinson and Willemsen [6] where $p_t + p_c = 0.66 + 0.31 < 1$.

In this paper estimates for trapping percolation thresholds on the triangular, square, simple-cubic, body-centered cubic, and face-centered cubic lattices are estimated by Monte Carlo simulations. These trapping thresholds appear to obey the universal formula proposed by Galam and Mauger [10] for ordinary percolation thresholds, but with different numerical values.

II. IMPLEMENTATION

For hypercubic networks, simulations were performed on $L \times L$ and $L \times L \times L$ lattices. The unit vectors for the body-centered cubic and face-centered cubic lattices were the same as used by Lorenz and Ziff [11], and the diamond lattice was also based on a cubic structure. Rhombic boundaries were used for the triangular network.

Simulations began by assigning an uncorrelated random number to each site from an arbitrary distribution. At each step the site with the largest value was chosen to be the next site to be occupied. Fluid was trapped when the displaced fluid became disconnected from a single face, designated the outflow face, and no further invasion into trapped regions was allowed. The other faces acted as trapping boundaries. Trapping was efficiently implemented by using the Hoshen and Kopelman cluster labeling algorithm [12] so that in the numerical code only one pass over the sites was required. Some speed improvement was obtained by running a check

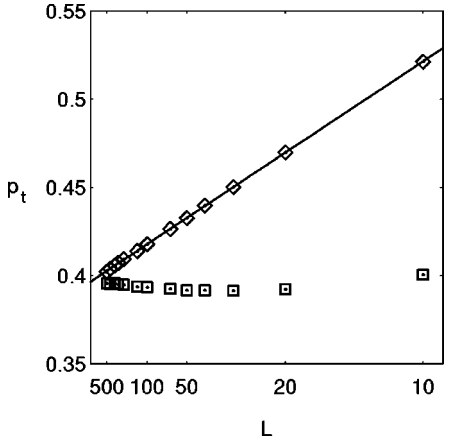

FIG. 1. Trapping thresholds $p_t(L)$ on a square ($q=4$) network plotted against L (abscissa scale is $L^{-0.77}$). Square and diamond symbols were obtained using rules $\mathfrak{R}_1$ and $\mathfrak{R}_2$, respectively.

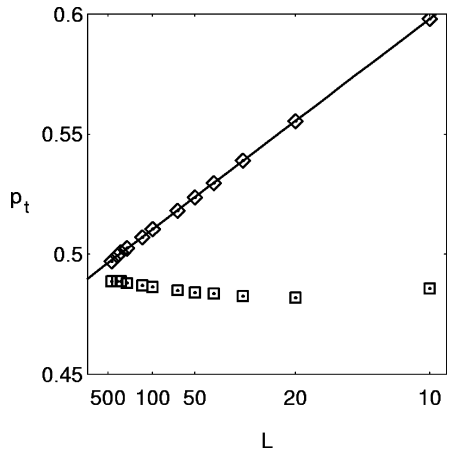

FIG. 2. Trapping thresholds $p_t(L)$ on a triangular ($q=6$) network plotted against L (abscissa scale is $L^{-0.72}$). Square and diamond symbols were obtained using rules $\Re_1$ and $\Re_2$, respectively.

in the local region as each site was added to detect the possibility of trapping occurring at that step. Only if trapping was a possibility was the full network searched. Between 10 and 10^5 realizations were run over a range of values of L, with a target standard error of $\leqslant 0.001$. The maximum size lattice simulated in 2D had $L=500$ and in 3D $L=80$. The simulations consumed an aggregate of some months of fast desktop CPU time.

The finite-size threshold $p_t(L)$ for the fraction of invading phase can be defined in various ways. Here two definitions were studied to provide additional estimates of accuracy: (a) the defending phase becomes disconnected from the face opposite the outflow face, rule $\Re_1$, and when (b) all the defending fluid is trapped, rule $\Re_2$. For all of the cases here, these two rules converge to the same value as $L\to\infty$.

III. RESULTS

Results of the numerical simulations are plotted in Figs. 1–6. Finite-size scaling for $p_t(L)$ was fitted to the relationship

$$p_t(L)-p_t=AL^{-y}. \tag{1}$$

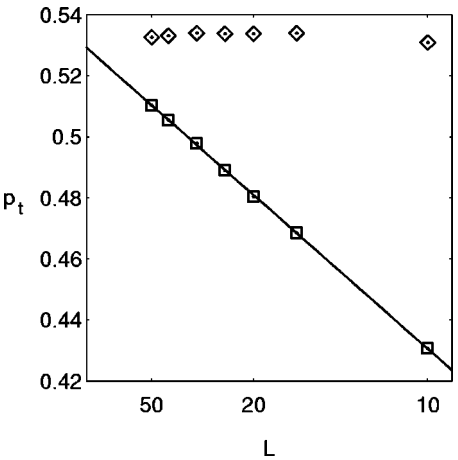

FIG. 3. Trapping thresholds $p_t(L)$ on a diamond ($q=6$) network plotted against L (abscissa scale is $L^{-1.03}$). Square and diamond symbols were obtained using rules $\Re_1$ and $\Re_2$, respectively.

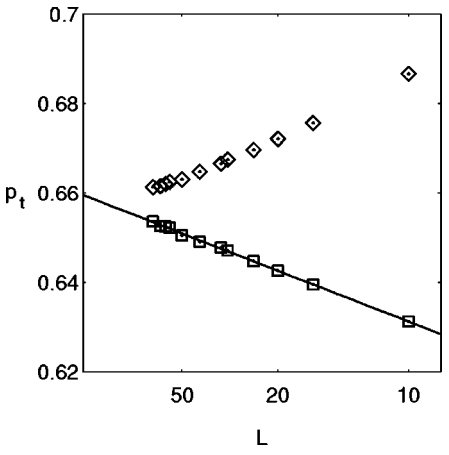

FIG. 4. Trapping thresholds $p_t(L)$ on a simple-cubic ($q=6$) network plotted against L (abscissa scale is $L^{-0.74}$). Square and diamond symbols were obtained using rules $\Re_1$ and $\Re_2$, respectively.

In two dimensions values produced using rule $\Re_1$ tended to follow Eq. (1) more closely, whereas in three dimensions rule $\Re_2$ appeared to give a better match. Fitted values for A and y are recorded in Table I. The y values were used to construct the abscissa scales in Figs. 1–6.

Extrapolated values for p_t as $L\to\infty$ are summarized in Table II, where known values of p_c are included for comparison. Also shown are the sums p_t+p_c. Note that the 2D lattices give $p_t>0$ as $L\to\infty$, unlike invasion percolation with trapping [6].

Galam and Mauger [10] have proposed the following single formula for the ordinary percolation threshold (without trapping) on all lattices:

$$p_c=p_0[(d-1)(q-1)]^{-a}d^b, \tag{2}$$

where d is the dimension and q is the coordination number. For site percolation Galam and Mauger estimate the values $\{p_0=0.8889;\ a=0.3601\}$ on the triangular, square, and honeycomb lattices, and $\{p_0=1.2868;\ a=0.6160\}$ on all lattices $d\geqslant 3$. For site percolation $b=0$. This relationship is not exact

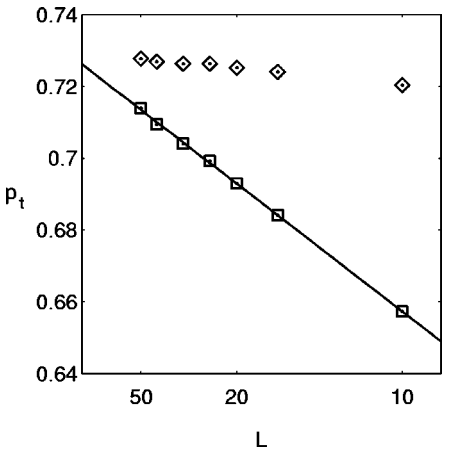

FIG. 5. Trapping thresholds $p_t(L)$ on a body-centered cubic ($q=8$) network plotted against L (abscissa scale is $L^{-1.05}$). Square and diamond symbols were obtained using rules $\Re_1$ and $\Re_2$, respectively.

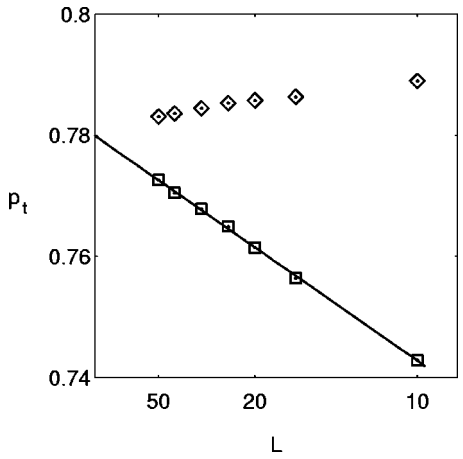

FIG. 6. Trapping thresholds $p_t(L)$ on a face-centered cubic ($q=12$) network plotted against L (abscissa scale is $L^{-1.01}$). Square and diamond symbols were obtained using rules $\mathfrak{R}_1$ and $\mathfrak{R}_2$, respectively.

and van der Marck [13] explores evidence that dimension and coordination number are not sufficient to predict percolation thresholds. Here the inexactness of the formula was tested against the limited range of p_c values in Table II. On the lattices with $d=2$ this gave $\{p_0=1.17;\ a=0.33\}$ and with $d=3$ $\{p_0=1.24;\ a=0.60\}$ was obtained. From Galam and Mauger [10] the values that deviate most from the formula are the square ($+0.0056$) and the body-centered cubic ($+0.007$) lattices, hence the deviation here from Galam and Mauger's values: they also included results from $d>3$.

It was of interest to test the trapping thresholds against Galam and Mauger's formula. The p_t values in Table II were fitted to

$$p_t=1-p_0[(d-1)(q-1)]^{-a}d^b \tag{3}$$

giving $\{p_0=1.17;\ a=0.33\}$ with $d=2$ and $\{p_0=1.33;\ a=0.59\}$ with $d=3$. A fit of the values in Table II to Eqs. (2) and (3) is shown in Fig. 7. Combining the p_t and p_c results allows a comparison of the difference between percolation thresholds with and without trapping:

$$1-p_t-p_c=0.02(q-1)^{-0.33}$$

in two dimensions and

$$1-p_t-p_c=0.06(q-1)^{-0.60}$$

in three dimensions.

TABLE I. Finite-size scaling for $p_t(L)$ given by Eq. (1), ordinary site percolation with trapping.

Lattice	A	y	Rule
Square ($d=2$, $q=4$)	0.73	0.77	$\mathfrak{R}_2$
Triangular ($d=2$, $q=6$)	0.57	0.72	$\mathfrak{R}_2$
Diamond ($d=3$, $q=4$)	−1.05	1.03	$\mathfrak{R}_1$
Simple cubic ($d=3$, $q=6$)	−0.16	0.74	$\mathfrak{R}_1$
Body-centered cubic ($d=3$, $q=8$)	−0.78	1.05	$\mathfrak{R}_1$
Face-centered cubic ($d=3$, $q=12$)	−0.38	1.01	$\mathfrak{R}_1$

TABLE II. Comparison of ordinary percolation thresholds and trapping thresholds. Accuracy estimates for p_t are better than ± 0.002.

Lattice	p_t	$p_c(site)$[a]	p_c+p_t
Square	0.396	0.5928	0.989
Triangular	0.490	0.5	0.990
Diamond	0.529	0.4299	0.959
Simple cubic	0.658	0.311604	0.970
Body-centered cubic	0.727	0.2460	0.974
Face-centered cubic	0.780	0.1998	0.980

[a]From Ref. [9], pp. 182–183.

IV. DISCUSSION

It can be concluded from this study that percolation with trapping appears to follow the same universal formula as the ordinary percolation threshold, with the same exponent a, but with a different coefficient p_0. In both 2D and 3D $p_t+p_c<1$ and $1-p_t-p_c\to 0$ as $q\to\infty$. This latter result is intuitively consistent with trapping becoming more difficult as the coordination number increases: there are more outlets for a potentially trapped fluid cluster to escape.

These results are significant because of the application to residual phases in multiphase flow through porous media and demonstrate the importance of coordination number. For reference, Sahimi [4] has remarked that for sandstones an average coordination number between 4 and 8 is a reasonable estimate. There are also unpublished measurements of carbonate rocks with coordination numbers in the range 2.3–4.4, although measurement of coordination number in real porous rocks is not subject to unambiguous interpretation, especially at these low coordination numbers.

Finally, some concluding observations on finite-size scaling can be made. For ordinary percolation without trapping, the exponent $-1/\nu$ appears, where ν is the correlation length exponent. ν has been determined as 4/3 in two dimensions and approximately 0.88 in three dimensions [2]. If the same

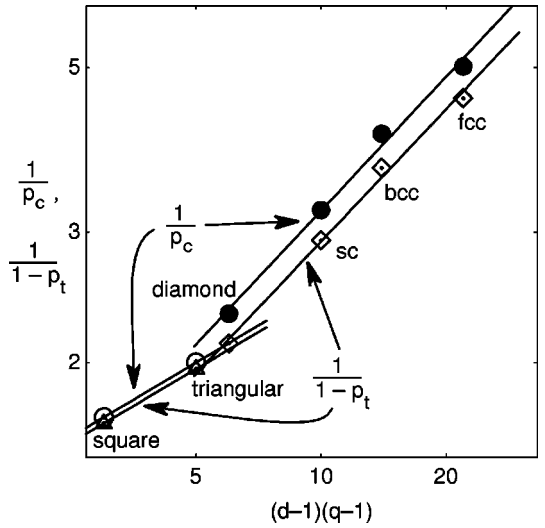

FIG. 7. Comparison of thresholds with and without trapping as a function of $(d-1)(q-1)$ with logarithmic scales. Circles and disks are for ordinary percolation without trapping, triangles and diamonds are for ordinary percolation with trapping.

scaling were to appear here, $y=0.75$ in two dimensions and $y=1.14$ in three dimensions would be expected. These values are close to, but different from, the values in Table I; noticeably different for the cubic lattice. It is difficult to draw conclusions because the estimates for the exponent y are not as good as p_t, and it is a problem to separate statistical scatter from deviations from Eq. (1) at small L values. Considerably more computational effort will be required to resolve the details of finite-size scaling for rules $\mathfrak{R}_1$, $\mathfrak{R}_2$ and alternative termination rules.

[1] J. Feder, *Fractals* (Plenum, New York, 1988).
[2] D. Stauffer and A. Aharony, *Introduction to Percolation Theory*, 2nd ed. (Taylor & Francis, London, 1994).
[3] M. Sahimi, *Applications of Percolation Theory* (Taylor & Francis, London, 1994).
[4] M. Sahimi, *Flow and Transport in Porous Media and Fractured Rock* (VCH, Weinheim, 1995).
[5] P. Meakin, *Fractals, Scaling and Growth Far From Equilibrium* (Cambridge University Press, Cambridge, England, 1998).
[6] D. Wilkinson and J. F. Willemsen, J. Phys. A **16**, 3365 (1983).
[7] M. M. Dias and D. Wilkinson, J. Phys. A **19**, 3131 (1986).
[8] M. Pokorny, C. Newman, and D. Meiron, J. Phys. A **23**, 1431 (1990).
[9] B. D. Hughes, *Random Walks and Random Environments* (Clarendon Press, Oxford, 1996), Vol. 2.
[10] S. Galam and A. Mauger, Phys. Rev. E **53**, 2177 (1996).
[11] C. D. Lorenz and R. M. Ziff, Phys. Rev. E **57**, 230 (1998).
[12] J. Hoshen and R. Kopelman, Phys. Rev. B **14**, 3438 (1976).
[13] S. C. van der Marck, Phys. Rev. E **55**, 1514 (1997).